

# Exergy Analysis of a Trigeneration System Driven by an Internal Combustion Engine with a Steam Ejector Refrigeration System

**M. Najafi\***

Department of Mechanical and Aerospace Engineering, Science and Research Branch, Islamic Azad University, Tehran, Iran

E-mail: M.najafi36@gmail.com

\*Corresponding author

**K. Javaherdeh**

Department of Mechanical Engineering, University of Gilan, Iran

E-mail: Javaherdeh@guilan.ac.ir

**B. Liravinia**

Department of Mechanical and Aerospace Engineering, Science and Research Branch, Islamic Azad University Tehran, Iran

E-mail: Behrouz\_Liravi@yahoo.com

Received: 11 December 2011, Revised: 27 June 2012, Accepted: 30 June 2012

**Abstract:** The present study analyzes a trigeneration system based on an internal combustion engine and a steam ejector refrigeration system from an exergy point of view. The present system is to produce cooling energy, heating energy and to supply power simultaneously. The analyses include a thorough implementation of the first law of thermodynamics and exergy formulations on each and every component of the designed cycle. Having computed the system exergy, the system exergy destruction sources are determined for both the summer and winter seasons. Based on the exergy analyses, about 360 kw by the internal combustion engine and about 70 kw by the steam generator are found to be the main exergy destruction sources in the cycle. Furthermore the heat generator and heat exchanger within the proposed cycle show to produce the maximum and minimum amount of exergy, respectively.

**Keywords:** Exergy Analysis, Gas Fired Engine, Steam Ejector Refrigeration System, Trigeneration

**Reference:** Najafi, M., Javaherdeh, K. and Liravinia, B., 'Exergy Analysis of a Trigeneration System Driven by an Internal Combustion Engine with a Steam Ejector Refrigeration System', Int J of Advanced Design and Manufacturing Technology, Vol. 5 /No. 3, 2012, pp. 61-71.

**Biographical notes:** **M. Najafi** received his PhD in mechanical engineering from the University of Alabama in 1989. His current research interests include energy storage systems, cooling systems, heating systems, mesh less numerical works in heat transfer and fluid flow in thermodynamic analysis. **K. Javaherdeh** received his PhD in mechanical engineering from University of Nancy in 1996. He is currently an assistant professor in the department of mechanical engineering, in Gilan University, Gilan, Iran. His current research interests include energy storage systems, cooling systems, design of heat exchangers, and optimization in thermodynamic analysis. **B. Liravinia** has received his master in mechanical engineering, from Science and Research Branch, Azad University, Tehran, Iran. His current research focuses on, thermodynamics and heat transfer.



pressure is decreased at the outlet of the nozzle and this pressure drop forces the generated steam to be sucked through the evaporator (secondary flow).

The primary and secondary flows are mixed together inside the ejector and the mixture enters a diffuser in order to provide the necessary pressure for exiting from the ejector and entering the condenser. After this stage, the flow in the condenser is condensed and a part of it is pumped into the heat generator by a pump and the process is repeated. The other portion of the condensed water, after passing through an expansion valve enters the evaporator to absorb the heat from the environment, and the cooling cycle is repeated again.

### 3 THERMODYNAMIC CALCULATIONS OF CYCLE COMPONENTS

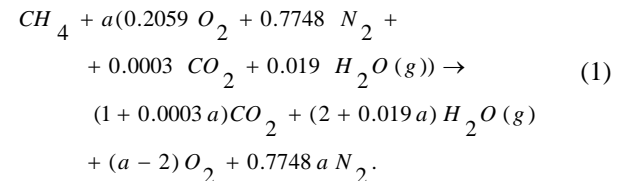
Assumptions used in this study are presented in Table 1.

**Table 1** Required assumptions for investigating performance of the cycle

Heat transfer from the engine to the environment	21 KW
environment air conditions in summer	T= 30 °C · P = 1bar
environment air conditions in winter	T= 10 °C · P = 1bar
Output power required from the engine	150 KW
Input energy to the engine	515 KW
Outlet gas Temperature from the engine	627 °C
Compression ratio of the engine	10
Heat transfer to the engine casing	178 KW
Evaporator temperature	12, 14, 16, 18 °C
Heat generator pressure	3, 4, 5, 6, 7 bar
Condenser temperature	42.5,45,50,52.5°C
HRSG pressure	15 bar
Efficiency of the ejector mixing part	1
Efficiency of the ejector nozzle	1
Efficiency of the ejector diffuser	0.5

### 3.1 GAS FIRED ENGINE – GENERATOR

First, the reaction carried out in the engine is considered [9,10]:



Variable  $a$  determines the amount of excess air in Eq. (1). It is necessary to write the first law for the engine to determine variable  $a$ :

$$Q_{c.v} - W_{c.v} = n_{CO_2} (\bar{h}_f^\circ + \Delta\bar{h})_{CO_2} + n_{H_2O(g)} (\bar{h}_f^\circ + \Delta\bar{h})_{H_2O(g)} + n_{O_2} (\bar{h}_f^\circ + \Delta\bar{h})_{O_2} + n_{N_2} (\bar{h}_f^\circ + \Delta\bar{h})_{N_2} - n_{CH_4} (\bar{h}_f^\circ + \Delta\bar{h})_{CH_4} - n_{O_2} (\bar{h}_f^\circ + \Delta\bar{h})_{O_2} - n_{N_2} (\bar{h}_f^\circ + \Delta\bar{h})_{N_2} - n_{CO_2} (\bar{h}_f^\circ + \Delta\bar{h})_{CO_2} - n_{H_2O} (\bar{h}_f^\circ + \Delta\bar{h})_{H_2O} \quad (2)$$

In Eq. (2)  $\bar{h}_f^\circ$  and  $\Delta\bar{h}$  are the formation enthalpy and the enthalpy difference between each mode assessed at the base conditions. Also,  $n$  is the number of moles. By finding the formation enthalpy ( $\bar{h}_f^\circ$ ) and enthalpy difference ( $\Delta\bar{h}$ ) using tables of thermodynamics, the unknown coefficients of reaction ( $a$ ) will be determined.

If a gas is composed of a mixture of two gases A and B, then [9]:

$$m_{tot} h_{tot} = m_A h_A + m_B h_B \rightarrow h_{tot} = \frac{m_A}{m_{tot}} h_A + \frac{m_B}{m_{tot}} h_B \quad (3)$$

Thus, for these two points, it can be written that,

$$h_2 = \frac{1}{m_2} (m_{CO_2} h_{CO_2} + m_{H_2O} h_{H_2O} + m_{N_2} h_{N_2} + m_{O_2} h_{O_2}) \quad (4)$$

where  $m$  is the mass. In Eq. (4), enthalpy of point 2 is calculated at the engine exhaust temperature. Now to calculate entropy, the gas mixture equation is needed [11]:

$$\bar{s}_{mix} = \sum_i y_i \bar{s}_i^* \quad (5)$$

$$\bar{s}_i^* = \bar{s}_{T_i}^\circ - \bar{R} \ln \frac{y_i P}{P_o} \quad (6)$$

In the above equation,  $\bar{s}_i^*$  is the specific entropy of component  $i$  in the mixture,  $y_i$  is the component mole fraction,  $P$  is total pressure, and  $\bar{s}_{T_i}^\circ$  is the specific entropy at the given temperature and base pressure. Using Eq. (5) and (6), the following equation can be stated:

$$\begin{aligned} \bar{s}_2 = & y_{CO_2} \left( \bar{s}_{T_2}^\circ - \bar{R} \ln \frac{y_{CO_2} P_2}{P_o} \right) + y_{H_2O} \left( \bar{s}_{T_2}^\circ - \bar{R} \ln \frac{y_{H_2O} P_2}{P_o} \right) \\ & + y_{O_2} \left( \bar{s}_{T_2}^\circ - \bar{R} \ln \frac{y_{O_2} P_2}{P_o} \right) + y_{N_2} \left( \bar{s}_{T_2}^\circ - \bar{R} \ln \frac{y_{N_2} P_2}{P_o} \right). \end{aligned} \quad (7)$$

In the above equation,  $s$  is the specific entropy,  $\bar{R}$  is the gas constant, subscripts  $o$  show environment conditions, and subscripts 1, 2, ... show points of cycle.

### 3.2 HEAT RECOVERY STEAM GENERATOR

As shown in Fig. 2, a heat recovery steam generator consists of three major parts: an economizer, an evaporator and a super-heater. Water enters the economizer and its temperature is increased to saturation temperature; water then enters an evaporator and is converted into saturated vapor, and then, to enter a super-heater it is converted into a superheated steam. Having the pinch point, (temperature difference of the inlet gas and outlet water from the economizer) the following equation can be written:

$$T_{2''} = T_{23'} + T_{\Delta Pinch} \quad (8)$$

where the subscripts indicate temperatures measured for various parts of Fig. 2. To calculate  $\dot{m}_{23}$ , the first law should be written for the economizer:

$$\dot{m}_2 (h_{2''} - h_3) \times \eta_{HRSG} = \dot{m}_{23} (h_{23'} - h_{23}). \quad (9)$$

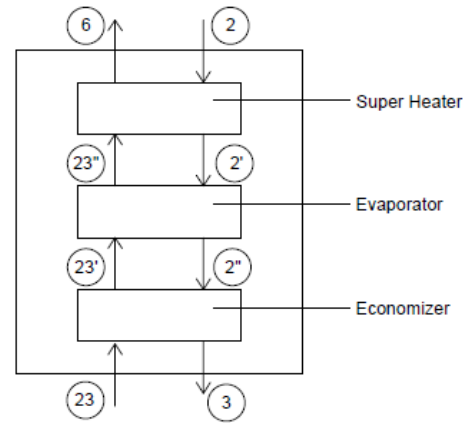


Fig. 2. Schematic view of various parts of heat recovery steam generator

Where  $\eta_{HRSG}$  is the efficiency of the heat recovery steam generator and  $\dot{m}$  is the mass flow rate of different components in the cycle. In Eq. (9),  $h_{2''}$  can be found based on the previous equation providing its temperature is known. To find  $h_6$  and its

corresponding temperature, the first law should be utilized for the super-heater.

Temperature of point  $2'$  is found based on trial and error. Such that an initial temperature is guessed for point  $2'$  (a temperature between 2 and  $2'$ ), then like the previous method (Eq. (4).),  $h_{2'N}$  is calculated at this temperature. Now, the calculated results should be compared with  $h_{2'}$  which was obtained from the general equation for the evaporator (Eq. (10).)

$$h_{2'} = \dot{m}_{23} \frac{(h_{23'} - h_{23'})}{\dot{m}_2 \eta_{HRSG}} + h_{2''} \quad (10)$$

If the difference is reasonable, then:

$$h_{2'N} = h_{2'} \quad (11)$$

**3.3 HEAT EXCHANGER NO. 1 (E.1)**

This heat exchanger is used only in winter. For analysis, writing the first law for heat exchanger No. 1 (E.1) is required [9]:

$$\dot{m}_7 (h_7 - h_{10}) \eta_{E.1} = \dot{m}_{21} (h_{22} - h_{21}), \tag{12}$$

**3.4 ANALYSIS OF STEAM EJECTOR REFRIGERATION SYSTEM**

Entrainment Ratio is the most important factor which is used to evaluate a steam ejector system (Fig. 3). To analyze this system, which works only in the summer, first the heat generator is examined. To find the mass flow rate, the enthalpy of the input and output to / from the heat generator, are required. Knowing that the given conditions of point 8 is quite similar to those of point 6, conditions of point 8 are defined and because the the conditions of points 9 and 23 are quite similar, the conditions of point 9 must be known. Assuming that pressure is 3bar for the heat generator, the enthalpy of point 11 which is the enthalpy of the saturated steam, is computed. To find enthalpy of point 17, the pump is analyzed. By writing the first law for the pump, enthalpy of point 17 is calculated as follows [9]:

$$\left. \begin{aligned} \dot{Q} - \dot{W} &= \dot{m} (h_{17} - h_{15}) \\ \dot{W} &= \dot{m} (P_{Enter} - P_{Exit}) v \end{aligned} \right\} \rightarrow h_{17} = h_{15} + \frac{(P_{Exit} - P_{Enter}) v}{\eta} \tag{13}$$

It should be noted that,  $P_{Enter}$  is the pressure of point 15 ( $P_{15}$ ) which is equal to the saturation pressure at the condenser outlet temperature,  $\dot{W}$  is rate of work, and  $\dot{Q}$  is rate of heat transfer. Now, by writing the first law for the heat generator (H.G),  $\dot{m}_{17}$  can be found [11]:

$$\dot{m}_8 (h_8 - h_9) = \dot{m}_{17} (h_{11} - h_{17}). \tag{14}$$

The conditions for point 16 and point 14 are also quite similar. Enthalpy is constant in the expansion valve, and the temperature of the evaporator is known. So knowing the saturation pressure at point 18, the pressure of point 18 can be found.

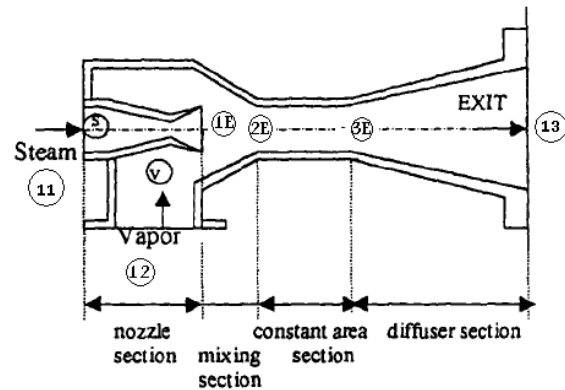


Fig. 3. Schematic view of an ejector

Considering these information, the following equations are used to analyze the ejector [9], [11], [12]:

$$x_{1E} = \frac{S_{11} - S_f @ P = P_{evap}}{S_{fg} @ P = P_{evap}} \tag{15}$$

$$h_{1ES} = h_f @ P = P_{evap} + x_{1E} h_{fg} @ P = P_{evap} \tag{16}$$

$$\frac{V_{1E}^2}{2} = \eta_n (h_{11} - h_{1ES}) \tag{17}$$

$$h_{1E} = h_{11} - \eta_n (h_{11} - h_{1ES}), \tag{18}$$

where the subscript s shows isentropic states, V stands for speed, x stands for quality, subscript f shows saturated liquid, subscript g shows saturated gas, subscript fg shows the difference between saturated liquid and vapor, subscript n shows nozzle condition, subscript evap shows evaporator condition, and subscript E stands for ejector. Having found  $h_{1ES}$ ,

$h_{1E}$  and  $V_{1E}$  the ratio of the mass flow rate belonging to point 12 to the mass flow rate belonging to point 11, denoted by 'W', follows[11]:

$$W = \frac{\dot{m}_{12}}{\dot{m}_{11}}. \tag{19}$$

It should be mentioned here that,  $\dot{m}_{11}$  is obtained from the present analysis for the heat generator. Using the following equation, it is concluded that, for  $V_{2E}$  [11]:

$$(\dot{m}_{11} + \dot{m}_{12})V_{2E} = \eta_m \dot{m}_{11} V_{1E}, \quad (20)$$

where subscript  $m$  indicates mixture. Using the following equation  $h_{2E}$  is obtained [11]:

$$(\dot{m}_{11} + \dot{m}_{12}) \left[ h_{2E} + \frac{V_{2E}^2}{2} \right] = \dot{m}_{12} h_{12} + \dot{m}_{11} \left[ h_{1E} + \frac{V_{1E}^2}{2} \right]. \quad (21)$$

Now, the speed of sound should be calculated [11]:

$$C_{2E} = \sqrt{K_{2E} R_{2E} T_{2E}}, \quad (22)$$

where  $C$  is the velocity of sound. If  $V_{2E} > C_{2E}$ , shock will occur (this generally develops in the ejector). Therefore, from [12]:

$$x_{2E} = \frac{h_{2E} - h_f @ P = P_{evap}}{h_{fg} @ P = P_{evap}} \quad (23)$$

$$Ma_{2E} = \frac{V_{2E}}{C_{2E}} \quad (24)$$

$$Ma_{3E}^2 = \frac{Ma_{2E}^2 + \frac{2}{k_{3E} - 1}}{\frac{2Ma_{2E}^2 \times K_{3E} - 1}{K_{3E} - 1}}, \quad (25)$$

where  $Ma$  is the Mach number.

Now,  $P_{3E}$  is obtained through the following equation [12]:

$$\frac{P_{3E}}{P_{2E}} = \frac{1 + K_{2E} Ma_{2E}^2}{1 + K_{3E} Ma_{3E}^2}, \quad (26)$$

where  $T_{3E}$  is also obtained through Eq. (27). [12]:

$$\frac{T_{3E}}{T_{2E}} = \frac{P_{3E} V_{3E}}{P_{2E} V_{2E}}, \quad (27)$$

and  $V_{3E}$  is obtained through Eq. (28). [12]:

$$\frac{T_{3E}}{T_{2E}} = \left( \frac{P_{3E}}{P_{2E}} \right)^2 \left( \frac{Ma_{3E}}{Ma_{2E}} \right)^2, \quad (28)$$

$C_{3E}$  can be obtained by Eq. (29). [11], [12]:

$$Ma_{3E} = \frac{V_{3E}}{C_{3E}}. \quad (29)$$

Finally, after using the above equations, enthalpy of point 13 is determined as [11]:

$$h_{13} = h_{3E} + \frac{V_{3E}^2}{2\eta_d}, \quad (30)$$

where subscript  $d$  stands for the diffuser. Considering the assumptions of most references, entropy of point 13 is equal to the entropy of point  $C_{3E}$ . Now, having two properties for point 13 (entropy and enthalpy), pressure for point 13 is obtained. Since the pressure drop in the condenser is assumed to be zero, the pressure for point 13 is equal to that of point 14. Now, the obtained pressure in the ejector is compared with the pressure of point 14. If there are obvious differences, the initial value for  $(\dot{m}_{12}/\dot{m}_{11})$  should be changed and the procedure should be repeated.

Thus, enthalpy, entropy and mass flow rate for all components of the cycle are hereby found. A program has been written in MATLAB software for the above process and for all iteration steps, using trial and error method.

#### 4 EXERGY ANALYSES

Equation (31) shows the total exergy for each component of the cycle, where  $e_k$ ,  $e_p$ ,  $e_{ch}$  and  $e_{ph}$  represent the kinetic, potential, chemical, and physical exergies, respectively.

$$e = e_{ph} + e_{ch} + e_p + e_k, \tag{31}$$

where  $e$  stands for specific exergy. For our purposes, in the above equation both the kinetic and potential exergies can be neglected, and physical and chemical exergies can be found as follows [10, 16]:

$$e_{ph} = (h - h_o) - T_o (S - S_o), \tag{32}$$

$$\bar{e}_{ch,mix} = \sum y_k \bar{e}_{ch,k} + \bar{R} T_o \sum y_k \ln y_k, \tag{33a}$$

$$\bar{e}_{ch,k} = -\bar{R} T_o \sum y_k \ln y_k^e, \tag{33b}$$

$$e_{ch,fuelGas} = LHV_{F.G} \left[ 1.033 + 0.0169 \frac{b}{a} - \frac{0.0698}{a} \right], \tag{34}$$

where LHV stands for low heating value. Based on the extended Matlab code, developed for the present study, exergy for all the states in Fig. 1 can now be determined as follows:

Equation (34) can be used to find chemical exergy for point 26 (Fig. 1). Should fuel enter the engine at the surrounding conditions, as Eq. (32) shows, the physical exergy becomes zero. Knowing that fuel enters the engine at the environment temperature, the only remaining exergy to be calculated for this point, would be chemical exergy.

For state 1, it is obvious that the physical and chemical exergies are zero. For state 2, to find the reference enthalpy and entropy for the exiting gases from the engine [16], first, the amount of water vapor in the product being liquefied to reach the surrounding temperature should be determined.

To do so, the water vapor partial pressure and its corresponding dew point temperature can be determined from the appropriate tables. Now, should the dew point temperature exceed the reference temperature, some of the available water vapor in the product will be condensed. For the remaining water vapor the following procedure [10] determines the amount of physical exergies for points 2 and 3 (Fig. 1):

$$P_v = \frac{n_v}{n_{CO_2} + n_{O_2} + n_{N_2} + n_v} P_2, \tag{35}$$

where  $n$ ,  $P_v$  and  $n_v$  are the number of moles, water vapor partial pressure at the reference temperature, and the Kmol of the vapor which is not condensed. Therefore, the number of moles for point 2 at the reference conditions and in vapor form is:

$$n_{2new} = n_{CO_2} + n_{O_2} + n_{N_2} + n_v. \tag{36}$$

$$y_{CO_2,new} = n_{CO_2} / n_{2,new}. \tag{37}$$

Now, to find  $\bar{h}_o$  and  $\bar{S}_o$ , the following equations are used:

$$\begin{aligned} \bar{h}_o = & n_{N_2} h_{N_2}(T_o) + n_{O_2} h_{O_2}(T_o) + n_{CO_2} \\ & h_{CO_2}(T_o) + n_v h_{H_2O(g)}(T_o) + n_{H_2O(L)} \\ & h_{H_2O(L)}(T_o), \end{aligned} \tag{38}$$

where subscript L indicates liquid, and  $n_v$  is the number of condensed moles. Also,

$$\begin{aligned} \bar{S}_o = & n_{N_2} S_{N_2}(T_o) + n_{O_2} S_{O_2}(T_o) + n_{CO_2} \\ & S_{CO_2}(T_o) + n_v S_{H_2O(g)}(T_o) + n_{H_2O(L)} \\ & S_{H_2O(L)}(T_o) - n_{N_2} \bar{R} \ln \frac{y_{N_2,New}^{P(2)}}{P_o} - n_{O_2} \bar{R} \\ & \ln \frac{y_{O_2,New}^{P(2)}}{P_o} - n_{CO_2} \bar{R} \ln \frac{y_{CO_2,New}^{P(2)}}{P_o} - n \\ & v \bar{R} \ln \frac{y_{v,New}^{P(2)}}{P_o}, \end{aligned} \tag{39}$$

where  $y_{New}$  is the mole portion at the reference condition. Using the above equation, the physical exergy for both points 2 and 3 (Fig. 1) can be determined. To find the chemical exergy for states 2 and 3, the following equations can be employed [10]:

$$\begin{aligned} e_{ch,2} = & [-\bar{R} T_o \left( y_{CO_2,New} \ln \left( \frac{0.0003}{y_{CO_2,new}} \right) + \right. \\ & \left. y_{O_2,New} \ln \left( \frac{0.2059}{y_{O_2,new}} \right) \right. \\ & \left. + y_{N_2,New} \ln \left( \frac{0.7748}{y_{N_2,new}} \right) \right) \\ & + y_{H_2O(g),New} \ln \left( \frac{0.019}{y_{H_2O(g),new}} \right) \Big] \\ & / M_{w,new,2} + n_{H_2O(L)} \frac{e_{CH,H_2O(L)}}{M_{W,H_2O}}, \end{aligned} \tag{40}$$

where M is the molecular weight. Also,

$$M_{w,new,2} = y_{CO_2,new} M_{w,CO_2} + y_{O_2,new} M_{w,O_2} + y_{N_2,new} M_{w,N_2} + y_{H_2O(g),new} M_{w,H_2O} \quad (41)$$

Now, using Eqs. (32) and (33), the physical and chemical exergies for the rest of the states in Fig. 1, can be found. Tables (2) and (3) show the physical, chemical, and total exergies for all the states indicated in Fig. 1. these tables are the results of the developed computer code for the present study. The standards used to evaluate the performance of the cogeneration systems are [13- 15]:

$$\varepsilon_{HRSG} = \frac{\dot{E}_6 - \dot{E}_{23}}{\dot{E}_2 - \dot{E}_3} \quad (42)$$

$$\varepsilon_{Ej} = \frac{\dot{E}_{13}}{\dot{E}_{11} - \dot{E}_{12}} \quad (43)$$

$$\varepsilon_{H.G} = \frac{\dot{E}_{11} - \dot{E}_{17}}{\dot{E}_8 - \dot{E}_9} \quad (44)$$

$$\varepsilon_{Evap} = \frac{\dot{E}_{20} - \dot{E}_{19}}{\dot{E}_{18} - \dot{E}_{12}} \quad (45)$$

$$\varepsilon_{E.1} = \frac{\dot{E}_{22} - \dot{E}_{21}}{\dot{E}_7 - \dot{E}_{10}} \quad (46)$$

$$\varepsilon_{motor} = \frac{\dot{W}_{net} + \dot{E}_5 - \dot{E}_4}{\dot{E}_{26} + \dot{E}_4 + \dot{E}_1} \quad (47)$$

where  $\varepsilon$  is exergy efficiency, Evap. stands for the evaporator, Ej stands for the ejector, and  $\dot{E}$  is the total rate of exergy. Exergy destruction rate for each component in Fig. 1, can be listed as,

$$\dot{i}_{HRSG} = \dot{E}_2 + \dot{E}_{23} - \dot{E}_3 - \dot{E}_6 \quad (48)$$

$$\dot{i}_{H.G} = \dot{E}_8 + \dot{E}_{17} - \dot{E}_9 - \dot{E}_{11} \quad (49)$$

$$\dot{i}_{cond.} = \dot{E}_{13} + \dot{E}_{24} - \dot{E}_{14} - \dot{E}_{25} \quad (50)$$

$$\dot{i}_{Evap.} = \dot{E}_{19} + \dot{E}_{18} - \dot{E}_{12} - \dot{E}_{20} \quad (51)$$

$$\dot{i}_{Ej} = \dot{E}_{11} + \dot{E}_{12} - \dot{E}_{13} \quad (52)$$

$$\dot{i}_{E.1} = \dot{E}_7 + \dot{E}_{21} - \dot{E}_{22} - \dot{E}_{10} \quad (53)$$

$$\dot{i}_{motor} = \dot{E}_{26} \left( 1 - \frac{\dot{W}_{net} + \dot{E}_5 - \dot{E}_4}{\dot{E}_{26} + \dot{E}_4 + \dot{E}_1} \right), \quad (54)$$

where  $\dot{i}$  is the rate of exergy destruction, and Cond. stands for the condenser.

## 5 RESULTS AND VALIDATIONS

After the above calculations, the following results are achieved through the developed computer code:

As Fig. (4a) and (4b) show, the internal combustion engine (Fig. 1) causes the maximum exergy destruction (irreversibility) in both summer and winter seasons, respectively.

**Table 2** Winter season exergy results (Fig. 1)

STATE	m (Kg/s)	T (°C)	P (bar)	h (Kj/Kg)	S (Kj/Kg °K)	$e_{ph}$ (Kj/Kg)	$e_{ch}$ (Kj/Kg)	$E_{tot}$ (Kj/Kg)
1	0.2263	10	1	276.5	6.8192	0	0	0
2	0.2365	600	10	1050.1	7.8313	3015.7	3015.7	724.8016
3	0.2365	167	9.5	507.6	7.6982	2510.9	2510.9	605.4163
4	0.7093	10	1	42.1	0.1511	0	0	2.128
5	0.7093	70	1	293.1	0.955	23.3	23.3	18.655
6	0.0484	297.85	15	3033	6.9115	1077.1	1077.1	52.2768
7	0.0484	297.85	15	3033	6.9115	1077.1	1077.1	52.2768
10	0.0484	100	15	420.1	1.3059	51	51	2.6136
21	0.5045	10	1	42.1	0.1511	0	0	1.5135
22	0.5045	70	1	293.1	0.955	23.3	23.3	13.268
23	0.0484	100	15	420.1	1.3059	51	51	2.614
26	0.0103	10	1	590.8	11.5146	0	0	532.593

Table 3 Summer season exergy results (Fig. 1)

STATE	$\dot{m}$ (Kg/s)	T (°C)	P (bar)	$h$ (Kj/Kg)	$S$ (Kj/Kg °K)	$e_{ph}$ (Kj/Kg)	$e_{ch}$ (Kj/Kg)	$E_{tot}$ (Kj/Kg)
1	0.2342	30	1	276.5	6.8662	0	0	0
2	0.2445	600	10	1050.1	7.8223	2904.1	49	722.033
3	0.2445	167	9.5	507.6	7.6911	2403.6	49	599.6607
4	1.0643	30	1	42.1	0.4368	0	3	3.1929
5	1.0643	70	1	293.1	0.955	10.2	3	14.0488
6	0.0499	297.63	15	3033	6.9107	944.6	3	47.2852
8	0.0499	297.63	15	3033	6.9107	944.6	3	47.2852
9	0.0499	100	15	420.1	1.3059	30.8	0	1.53692
11	0.0514	133.5254	3	2724.9	6.9916	612	3	31.611
12	0.0128	12	0.014	2522.9	8.8514	-153.8	3	-1.93024
13	0.0642	237.1558	0.0963	2952.2	9.0702	209.2	3	13.62324
14	0.0642	45	0.0959	188.4	0.6386	1.4	3	0.28248
15	0.0514	45	0.0959	188.4	0.6386	1.4	3	0.22616
16	0.0128	45	0.0959	188.4	0.6386	1.4	3	0.05632
17	0.0514	45	3	188.4	0.6386	1.4	3	0.22616
18	0.0128	12	0.014	188.4	0.6647	-6.5	3	-0.0448
19	0.448	30	1	125.8	0.4368	0	3	1.344
20	0.448	14	1	58.9	0.2099	1.8	3	2.1504
23	0.0499	100	15	420.1	1.3059	30.8	3	1.68662
24	0.8488	30	1	125.8	0.4368	0	3	2.5464
25	0.8488	80	1	335	1.0754	15.6	3	15.78768
26	0.0103	30	1	636	11.6775	0	51708	532.593

Figures (5a) and (5b) show the exergy efficiency for different components of Fig. 1, for summer and winter seasons, respectively. As Fig. (5a) indicates, for the summer season, the heat generators and the engine have the highest and lowest exergies, respectively. Also as Fig. (5b) shows, for the winter season, the heat recovery steam generator and number 1 heat exchanger (Fig. 1) have the highest and lowest exergies,

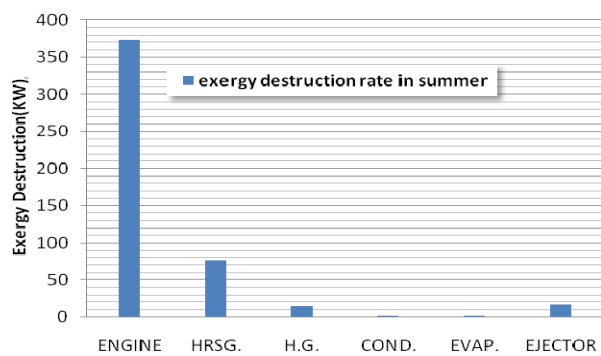


Fig. 4a Exergy destruction rate for different components of Figure 1 during summer

respectively. As Fig. 6 from reference [17] shows, in their study like the present work in Figs. (4a) and (4b), the maximum exergy destruction belongs to the internal combustion engine and heat recovery steam generators. Again, Figs (4a) and (4b) in this study like Fig. 6 by [17] agree that the least exergy destruction belongs to the condenser and evaporator. These comparisons prove the validity of the present work.

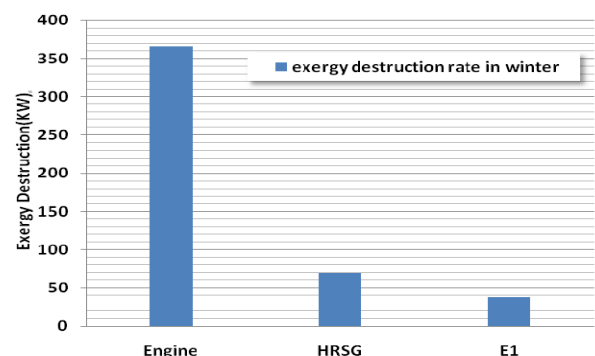
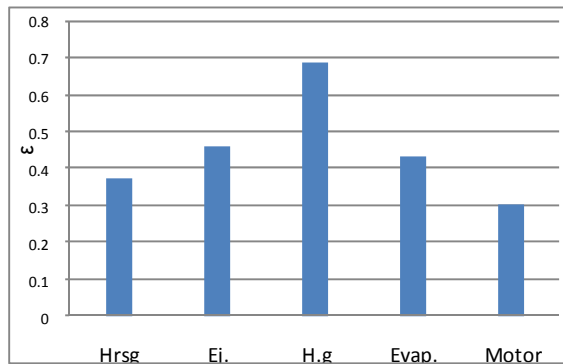
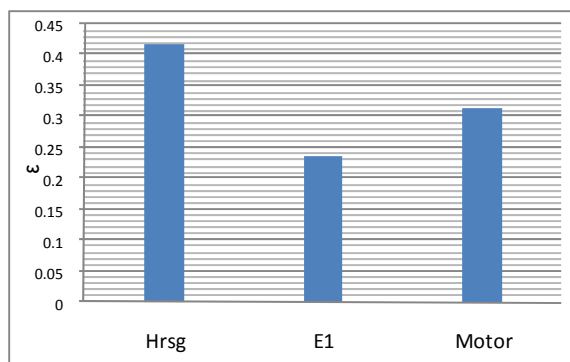


Fig. 4b Exergy destruction rate for different components of Figure 1 during winter



**Fig. 5a** Exergy generation for different components of Figure 1 during summer



**Fig. 5b** Exergy generation for different components of Figure 1 during winter

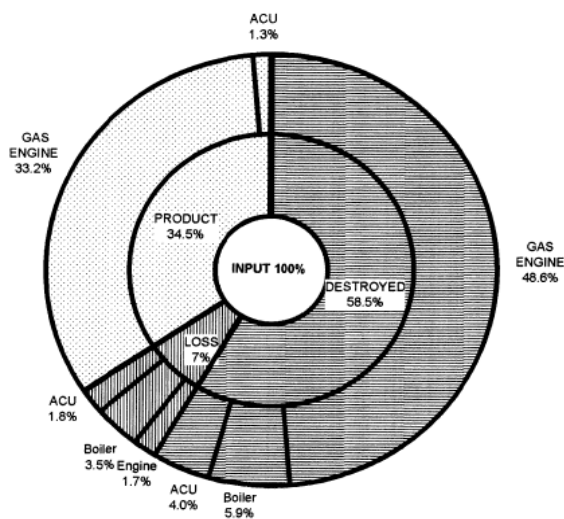


**Fig. 6** Exergy distribution for a simultaneous energy generation cycle's components

## 6 CONCLUSIONS AND DISCUSSIONS

In the present study, a simultaneous energy generation cycle for cooling, heating and power supplying is designed and each component of the system is analyzed from thermodynamic and exergy aspects. The maximum and minimum exergy generation as well as the maximum and minimum exergy destruction by the components for both the summer and winter cycles are distinguished, and are validated through comparisons made with the appropriate results of another investigator. Based on the exergy analyses, the internal combustion engine and the heat recovery steam generator prove to be the most exergy destroying sources by about 360 KW and 70 KW, respectively. The highest and lowest exergy production sources prove to be the heat generator and the heat exchanger, respectively.

In general, utilizing a simultaneous energy generation system definitely invites economic advantage. However, selection of the appropriate capacity for each cycle component plays an important role in achieving this advantage, and needs much experimental as well as analytical study as future work.

## ACKNOWLEDGEMENTS

The authors would like to thank the Iranian fuel conservation company (IFCC) for sponsoring this research project.

## REFERENCES

- [1] Comprehensive guide to the cogeneration of electricity and heat, The office of improving optimization and economy of energy and electricity of Energy Ministry, 1388, Tehran.
- [2] Khaliq A., "Exergy analysis of gas turbine trigeneration system for combined production of power heat and refrigeration", International Journal of Refrigeration, No. 32, 2009, pp. 534 – 545.
- [3] Wu, D. W. and Wang, R. Z., "Combined cooling, heating and power: A review", progress in energy and combustion science, No. 32, 2006, pp. 459 – 495.
- [4] Kong, X. Q. and Wang, R. Z. "Experimental investigation of a micro-combined cooling, heating and power system driven by a gas engine", International Journal of Refrigeration, No. 28, 2005, pp. 977 – 987.
- [5] Kanoglu M. and Dincer I., "Performance assessment of cogeneration plants", energy conversion and management, No. 10, 29 Aug. 2008, pp. 10 – 16.
- [6] Yiping Dai et al., "Exergy analysis, parametric analysis and optimization for a novel combined power and ejector refrigeration cycle", applied thermal engineering, No. 10, 16 Sep. 2008, pp. 10 – 16.

- [7] Cardona E. and Piacentino A., "Optimal design of CHCP plants in the civil sector by thermoeconomics", *applied energy*, No. 84, 2007, pp. 729 – 748.
- [8] Ganapathy V., ABCO industries abilene, industrial boilers and heat recovery steam generators design, applications, and calculations, marcel dekker, Inc. New York, 2003, ISBN: 0-8247 – 0814 – 8.
- [9] Rober H. Perry, Perry's chemical engineers' handbook, 7<sup>nd</sup> ed., McGraw-Hill, 1999, ISBN: 0 – 07 – 049841 – 50.
- [10] Bejan A., Tsatsaronis G., Morn M., Thermal design and optimization, john willey-interscience publication, New York, 1996, ISBN: 0 – 471 – 58467 – 30.
- [11] Narmine H. Aly, Karameldin Aly and Shamloul, M. M., "Modelling, and simulation of steam jet ejectors", *desalination*, No. 123, 1999, pp. 1 – 8.
- [12] Cengel, Yunus A., Boles, Michael A., Thermodynamic an engineering approach, 5<sup>nd</sup>ed., McGraw-Hill. 1997.
- [13] Feng, X., Cai, Y. N. and Qian, L. L., "A new performance criterion for cogeneration system", *energy conversion and management*, Vol. 39, No. 15, 1998, pp. 1607 – 1609.
- [14] Ozgur B., Haydar A. and Arif H., "Thermodynamic and thermoeconomic analyses of a trigeneration (TRIGEN) system with a gas–diesel engine: Part II – An application", *energy conversion and management* (to be published).
- [15] Ameri M., Behbahaninia A. and Tanha A. A., "Thermodynamic analysis of a tri-generation system based on micro-gas turbine with a steam ejector refrigeration system", *energy*, No. 35, 2010, pp. 2203 – 2209.
- [16] Ozgur B., Haydar A. and Arif, H., "Thermodynamic and thermoeconomic analyses of a trigeneration (TRIGEN) system with a gas–diesel engine: Part I – Methodology", *energy conversion and management*, Vol. 51, Issue 11, November 2010, pp. 2252–2259.
- [17] Galip T. and Durriye B., "Thermoeconomic analysis of a trigeneration system", *applied thermal engineering* 24, 2004, pp. 2689 – 2699.